



Thin film thickness measurements using Scanning White Light Interferometry

B. Maniscalco, P.M. Kaminski, J.M. Walls *

Centre for Renewable Energy Systems Technology, (CREST), School of Electronic, Electrical and Systems Engineering, Loughborough University, Leicestershire LE11 3TU, UK

ARTICLE INFO

Article history:

Received 11 December 2012

Received in revised form 28 September 2013

Accepted 2 October 2013

Available online 11 October 2013

Keywords:

Scanning White Light Interferometry

Coherence correlation interferometry

Thin film

Metrology

Thin film thickness

Surface roughness

Helical complex field

Ellipsometry

ABSTRACT

Scanning White Light Interferometry is a well-established technique for providing accurate surface roughness measurements and three dimensional topographical images. Here we report on the use of a variant of Scanning White Light Interferometry called coherence correlation interferometry which is now capable of providing accurate thickness measurements from transparent and semi-transparent thin films with thickness below 1 μm . This capability will have many important applications which include measurements on optical coatings, displays, semiconductor devices, transparent conducting oxides and thin film photovoltaics. In this paper we report measurements of thin film thickness made using coherence correlation interferometry on a variety of materials including metal-oxides (Nb_2O_5 and ZrO_2), a metal-nitride ($\text{SiN}_x\text{:H}$), a carbon-nitride ($\text{SiC}_x\text{N}_y\text{:H}$) and indium tin oxide, a transparent conducting oxide. The measurements are compared with those obtained using spectroscopic ellipsometry and in all cases excellent correlation is obtained between the techniques. A key advantage of this capability is the combination of thin film thickness and surface roughness and other three-dimensional metrology measurements from the same sample area.

© 2013 Elsevier B.V. All rights reserved.

1. Introduction

Thin film thickness measurements with sub-nanometre accuracy are important in a range of applications such as thin film optical coatings, displays, semiconductor devices, thin film photovoltaics, thin film transparent conducting oxides For example, the precise thickness of a single layer anti-reflection coating determines its anti-reflective quality and spectral response. The precise thickness of a transparent conducting oxide will determine its transmittance and sheet resistance. Spectroscopic ellipsometry is usually used to make these measurements.

Likewise, surface roughness and other surface metrology measurements such as feature width, form, volume and angle on thin films are also important. In optical coatings, surface roughness causes scattering and haze. In display or photovoltaic devices, roughness of the transparent conducting oxide contact can lead to shunting of the devices. These metrology measurements are made using a variety of techniques including stylus profilometry, Atomic Force Microscopy, Scanning Electron Microscopy and Scanning White Light Interferometry (SWLI).

Here we report on the use of a variant of SWLI called coherence correlation interferometry (CCI) [1] which is now capable of combining sub-nanometre thin film thickness measurements with quantitative three-dimensional metrology and imaging from the same thin film sample area. The technique provides these measurements quickly and

accurately and now has a potentially important role not just in research and development but also in quality control in a manufacturing environment. The SWLI technique has previously been used routinely for thick film thickness measurements where the film is typically $>1 \mu\text{m}$. Although it has been recognised that combining thin film thickness measurements with surface metrology is a powerful capability, this has previously involved hardware modifications such as the addition of a polariser, a change of lens and also requires modelling software [2]. In this paper, we report on the use of a thin film measurement capability made possible by the development of the 'helical complex field' (HCF) function [3–6].

The HCF function equates to a topographically defined helix modulated by the electrical field reflectance of the film. As such, it provides a 'signature' of the thin film structure so that through optimization, the thin film structure may be determined on a local scale. In order to use the HCF function approach, it is necessary to provide an "a priori" knowledge of the dispersive film index. These values of refractive index (n) and the extinction coefficient (k) can be measured using ellipsometry or assumed from published bulk values. A "pattern" measurement can be performed for an accurate characterization of thickness uniformity. Although both ellipsometry and CCI rely on n and k to describe the dielectric function, the derivations are different since ellipsometry uses polarisation and CCI uses interference for the thickness measurement.

A variety of thin films have been investigated including metal-oxides, niobium pentoxide (Nb_2O_5) and zirconium oxide (ZrO_2), a metal-nitride ($\text{SiN}_x\text{:H}$), carbon-nitride ($\text{SiC}_x\text{N}_y\text{:H}$) and indium tin oxide (ITO) a transparent conducting oxide. The thin film thickness measurements

* Corresponding author.

E-mail address: J.M.Walls@lboro.ac.uk (J.M. Walls).

are compared with those obtained using spectroscopic ellipsometry and corresponding surface roughness measurements from the same sample areas are also presented.

2. Coherence correlation interferometry (CCI)

Coherence correlation interferometry (CCI) is a Scanning White Light Interferometry technique which uses light interference patterns (set of interference fringes) from a white light source (xenon). Two beams are produced by splitting the main beam from the source; one is reflected by a reference mirror, while the other one scans the surface. The light is reflected locally by the surface and the reflected beam is correlated to the reference one and an interference pattern is created. The signal is detected by a high resolution digital CCD camera. Three-dimensional topographical maps are created by measuring the position of the lens which is moved in the vertical direction to obtain the maximum constructive interference. Use of white light allows only one peak as maximum. Each pixel acts as single interferometer, combining them together allows the accurate measurement of a relatively large surface area. The accuracy of the measurement is highly dependent on the efficacy of the coherence correlation algorithm used.

One of the main advantages of the technique is that it is non-contacting and there is no risk of damaging the surface with a stylus. It also provides information in three dimensions which provides a more complete surface representation than two dimensions. Furthermore the measurements are taken over a relatively large and hence representative area of the surface. The scan area is defined by the magnification of the lens used and it ranges between 165 μm × 165 μm for a 100× objective lens to 6.6 mm × 6.6 mm for a 2.5× objective lens. The area can be further extended using “stitching mode” to combine images. It has the capability of obtaining measurements with sub-nanometre interferometric resolution with a vertical range limited at 100 μm by the vertical traverse available to the lens. The technique provides sub-micron lateral resolution depending on the wavelength of light and the numerical aperture (NA) of the objective. The technique provides two and three-dimensional images of the surface together with a range of quantitative analysis routines for roughness, waviness and form. Measurements include root mean square roughness (Sq), average roughness (Sa), maximum peak height (St), step height, groove width and depth, etc.

3. Thick and thin film thickness measurement analysis

Interference occurs when two light waves interfere; the resultant wave has an amplitude dependent on their phase difference. If the phase difference is 2mπ (where m is any integer), constructive interference occurs and the intensity is at a maximum. For the phase difference of (2 m + 1)π destructive interference occurs and the intensity is minimal. For the analysis of relatively thick films, typically greater than 1 μm, the interaction of the incident white light and the thin film surface and its interface results in the local formation of two distinct interference bunches. It is possible to locate the positions of the two envelope maxima and thereby determine the thick film thickness using refractive index information.

In the case of a transparent thin film, due to the proximity of the surface and the thin film interface, the interference bunches associated with the surface and the thin film overlap. The overlap of the interference bunches makes the film thickness measurement impossible using the traditional approach used for thick films which requires their separation. In this regime, it is necessary to operate with another approach using the ‘helical complex field’ (HCF) function.

The HCF function is based on a ‘reference’ material (defined by the input of n and k values) and the measured thin film. The net field reflectance of the ‘reference’ material $\overline{r}_{eff}(v)$ is multiplied by the ratio of the positive arm sidebands (SB⁺) of the Fourier transform of the interference intensities of the film and the ‘reference’ material.

\overline{z}_{xy} is the average difference between the two beams, \overline{z}_k is the average net path length shift of the sample of the kth step, the $I_{thin}(\overline{z}_k)$ is the interference intensity. The resulting HCF function is spatially defined as a distorted helix, which is modulated by the electrical field of reflectance of the film.

$$HCF(v) = \overline{r}_{eff}(v) \frac{F^-(I_{thin}(\overline{z}_k))_{SB^+}}{F^-(I_{ref}(\overline{z}_k))_{SB^+}} = a_{HCF}(v) e^{i\varphi_{HCF}(v)}$$

This equation is the synthesized HCF function, which is referred to the dispersive index (n and k values). These values have to be inserted in the material data base prior to the measurement. They can be extracted from ellipsometry results or assumed from bulk values available in the literature; n and k are considered for a certain number of wavelength values mainly across the visible spectrum (350 nm–850 nm) and they refer to I_{ref} value in the HCF equation.

$F^-(I_{thin}(\overline{z}_k))_{SB^+}$ refers to the measured thin film, while $F^-(I_{ref}(\overline{z}_k))_{SB^+}$ depends on the input of the ‘reference’ material. The resulting function is expressed as helix function ($e^{i\varphi_{HCF}(v)}$) distorted by the term $a_{HCF}(v)$. The synthesized HCF function is then compared to the defined function. $r(v)e^{i\varphi(v)}$ is the electrical field reflectance and Δz_{HCF} is the difference between the position of the reference and the closest step of the scan.

$$HCF_{fit}(v) = \overline{r(v)} e^{i\varphi(v)} e^{i4\pi v \Delta z_{HCF}}$$

$HCF_{fit}(v)$ is used to fit $HCF(v)$ as shown. The lower the fitting number, the more accurate is the thickness measurement.

$$HCF(v) \cong HCF_{fit}(v) = a_{HCF}(v) e^{i\varphi_{HCF}(v)} \cong \overline{r(v)} e^{i\varphi(v)} e^{i4\pi v \Delta z_{HCF}}$$

Fitting figures reveal the validity of the measurement. An example is shown in Fig. 1. The continuous line represents $HCF_{fit}(v)$, the fitting function while the dotted line is $HCF(v)$, the synthesised function. The HCF approach can be broken down into three different parts, which identify the fitting figure for the CCI thin film measurement; the real part of the HCF is in red, the imaginary part of HCF is in blue and the reflectance is in green. The values are taken on the sampling profile from 0.8 mm to –0.8 mm across the field of view, against the wavelength of light in μm. Fig. 1 shows a good fitting of 0.198 for a 68.8 nm thin film of silicon carbon-nitride deposited on polished silicon. Better fittings were obtained for the thin films presented in this study, such as 0.018 for 67.6 nm thick silicon nitride coated on polished silicon,

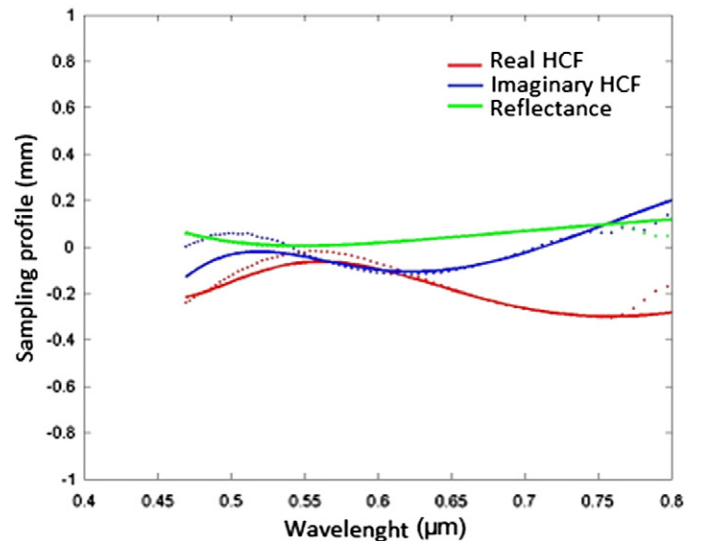


Fig. 1. Example of fitting figure (fit 0.198) of HCF function for 68.8 nm thick silicon carbon-nitride deposited on polished silicon.

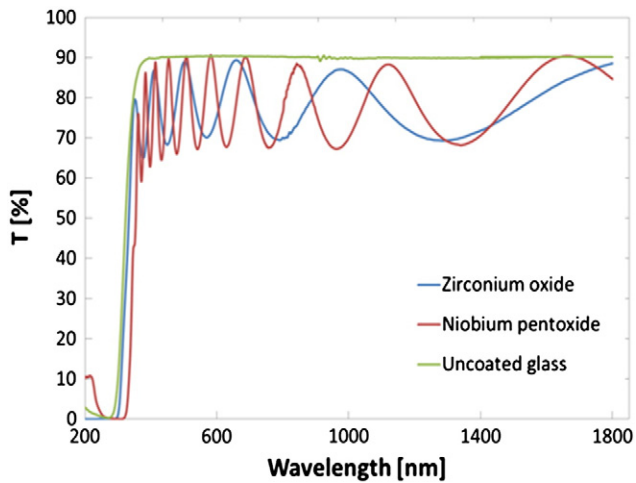


Fig. 2. The optical transmission of thin films of niobium pentoxide and zirconium oxide over a wavelength range from 200 nm to 1800 nm.

but the small disparity in this measurement helps to illustrate the method.

Excessive roughness introduces uncertainty in the thin film thickness measurements for both CCI and ellipsometry. This division of the interference sequence into both thin film and topography is only made possible because of the accurate values for n and k . If a thin film exhibited excessive surface roughness which significantly reduced the interference within the film, then the apparent n and k as determined by the ellipsometry will differ from the true values. Under these circumstances, it would be preferable to refer to dispersion from bulk reference values.

4. Thin film measurements

In this study, the thin film thickness measurements were made using a Sunstar HD CCI instrument from Taylor Hobson Ltd. These measurements were then compared for each thin film, using spectroscopic ellipsometry (Horiba Jobin Yvon UVISSEL iHR320FGAS). The spectroscopic ellipsometry measurements were also used to obtain refractive index (n) and extinction coefficient (k). Ellipsometry measures the change in the polarisation of the light upon reflection from the thin film layer [7]. Modelling allows the information to be translated to the refractive index dispersion over the spectral range. Spectroscopic ellipsometry works in a wide spectral range from the ultra violet to the infra-red (200 nm to 2.1 μm). It provides information about the real and imaginary part of refractive index and provides thin film thickness information with sub-nanometre precision.

The optical properties of the deposited films were measured with a spectrophotometer (Varian UV 5000). This instrument provides transmission spectra across a range of wavelengths. It is equipped with an integrating sphere and a set of gratings which allow the collection of information from wavelengths in the range 170 nm to 3.1 μm . For ITO, sheet resistance is a critical measurement. A four point probe is used to determine the average sheet resistance.

5. Results

Five thin films of increasing thickness were deposited for each material used in this study in the range 50 nm to 1 μm . The thickness of the thin films was then measured using CCI and spectroscopic ellipsometry. The CCI was also used to measure surface roughness and to provide a three dimensional topographical image to demonstrate the powerful combination of these measurements. These results are presented for each of the thin film materials. The thin film thickness measurements are compared graphically to determine the correlation between the two sets of data. The transmission of each material deposited on glass obtained using a spectrophotometer is also provided as a reference. The sheet resistance of the ITO films is also reported since this is dependent on film thickness.

6. Metal-oxides: ZrO_2 and Nb_2O_5

Dielectric metal-oxides such as zirconium oxide (ZrO_2) and niobium pentoxide (Nb_2O_5) are used extensively in multilayer optical coatings as the high index layer with Silica (SiO_2) almost always used as the low refractive index material. For example, this combination of materials is commonly used to deposit multilayer anti-reflective (AR) coatings. The refractive index of magnetron sputtered thin films can approach that of the bulk material. For zirconium oxide, this is $n = 2.1$ at 550 nm while that of niobium pentoxide is $n = 2.37$ which when used together with the low refractive index for silicon dioxide, which is typically $n = 1.47$, make a good pairing for to obtain a high quality AR coating. In general, the greater the difference in refractive index between alternate layers in a multilayer design, the better the optical performance. In an AR coating this is evident in the reduced reflection loss [8]. Accurate thickness determination of each layer in a multilayer AR coating provides essential measurements for the analysis of optical performance [9]. For this study, a range of thin film reference samples were prepared by reactive magnetron sputtering using a PV Express anti-reflection coating system from Power Vision Ltd. The thin films were deposited using a pulsed dc power supply (5 kW Pinnacle Plus, Advanced Energy Inc). The glass substrates were mounted on a vertical carrier rotating at 120 rpm past two six inch circular magnetrons and a reactive plasma source.

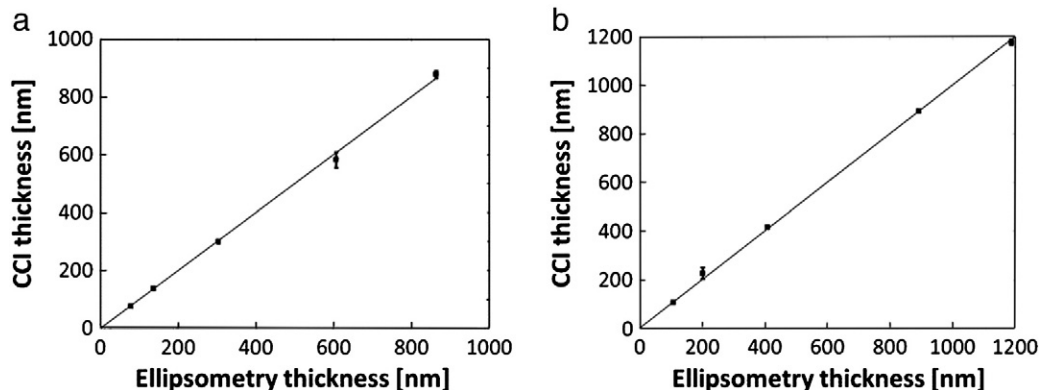


Fig. 3. Comparison between thin film thickness measurements obtained using ellipsometry and CCI techniques for a) niobium pentoxide thin films sputter-deposited on glass ($R^2 = 0.997$); b) zirconium oxide thin films sputter-deposited on glass ($R^2 = 0.999$).

A representative sample for each of these materials was selected to present optical measurements of transmittance across a wavelength range from 250 nm to 1800 nm.

Five niobium pentoxide thin films were deposited on soda lime glass substrates with a range of thicknesses from 70 nm to 1000 nm. A transmission spectrum from a 870 nm thick niobium pentoxide film is presented in Fig. 2. The film shows high transmission over a wide wavelength range, from 365 nm to 1800 nm. The film is transparent across the whole visible range, with interference fringes across the spectrum. The absorbance peak is around 365 nm, where the transmittance drops dramatically to zero.

A similar transmittance was measured for the thin film zirconium oxide on soda-lime glass samples. Interference fringes occur across the whole spectrum down to the absorption peak at 355 nm. The transmittance is high through the wavelength range from near-infrared and then it drops in the near-Ultra-Violet range. Both these materials are used in high quality anti-reflection coatings on ophthalmic lenses and in a range of precision optical applications.

Thin film thickness measurements were obtained using the CCI and the results compared with those obtained using spectroscopic ellipsometry. The measurements from the two techniques show excellent correlation for both niobium pentoxide and zirconium oxide. The results for niobium pentoxide are presented in Fig. 3a). The thickness range is from 70 nm to 1000 nm.

Fig. 3a) shows CCI measurements plotted against ellipsometry measurements. The line showing perfect correlation was plotted for reference. The coefficient of determination between the line and measured points is $R^2 = 0.997$ showing near perfect correlation.

The thickness measurements of five zirconium oxide thin films are presented in Fig. 3b), for a range of thicknesses from 70 nm to 1200 nm. R^2 for this set of measurements is 0.999, providing excellent correlation between the two techniques.

The CCI was also used to provide surface roughness measurements from each of the samples and from the same area. There are several roughness parameters in use. However, the most commonly used parameter for optical applications is the root mean square roughness (RMS) or Sq:

$$Sq = \sqrt{\frac{1}{n} \sum_{i=1}^n y_i^2}$$

Sq represents the root mean square of vertical deviations of the roughness profile from the mean line. CCI provides both three dimensional topographical images of the film surface and quantitative roughness measurements.

The surface maps obtained from sputter deposited thin films of niobium pentoxide and zirconium oxide are shown in Fig. 4. The

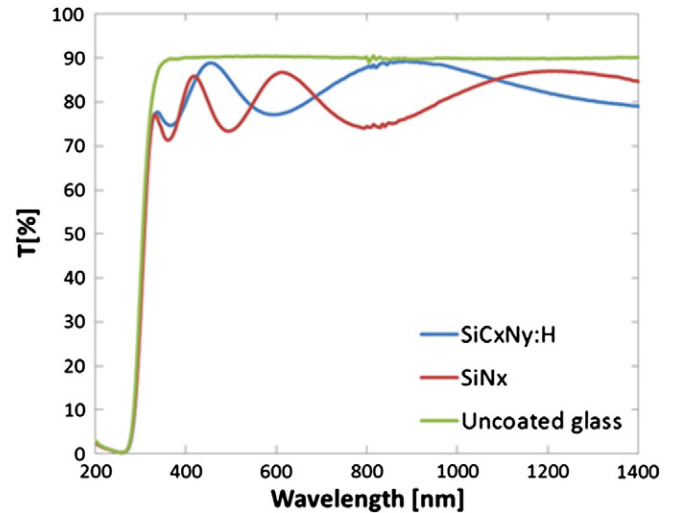


Fig. 5. The optical transmission spectra of silicon nitride and silicon carbon-nitride thin films deposited on glass.

niobium pentoxide thin film was 74.9 nm thick and was extremely smooth with a measured rms roughness of 1.2 nm. For comparison, the sputter-deposited zirconium oxide thin film is much thicker with a measured thickness of 893 nm. This thin film is also extremely smooth with an RMS roughness of 2.6 nm. These thin films are ideal for optical coating applications.

The CCI technique allows roughness to be measured as a function of thin film thickness. These optical quality films at all thicknesses were extremely smooth. The roughness generally increases with thin film thickness although niobium pentoxide films were slightly rougher when thickness exceeded 600 nm. For example, the RMS roughness of a thin film of thickness 900 nm was measured to be ~5 nm while the zirconium oxide of comparable thickness (shown in Fig. 4) had an RMS roughness of only 2.6 nm.

7. Silicon nitride (SiN_x :H) and silicon carbon-nitride (SiC_xN_y :H)

Anti-reflective coatings are also used for photovoltaic applications. Thin film coatings play a crucial role in silicon solar cell operation. Thin films are used to prepare anti-reflective coatings for the solar cell to reduce energy loss caused by reflection due to silicon-glass refractive index mismatch. The coating layer also plays a crucial role for surface passivation of the front side and in more advanced devices the rear

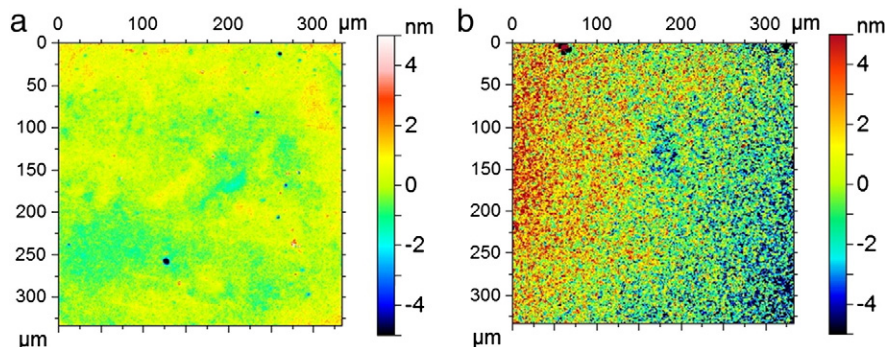


Fig. 4. A surface map – CCI images obtained from (a) 74.9 nm of niobium pentoxide with RMS roughness of 1.2 nm; (b) 893.4 nm thin film of zirconium oxide. The RMS roughness parameter Sq = 2.6 nm.

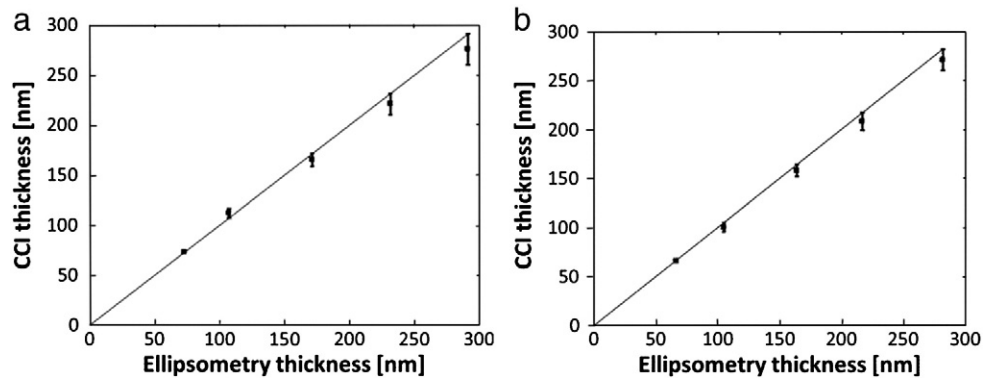


Fig. 6. Comparison between thin film thickness measurements obtained using ellipsometry and CCI techniques for a) silicon nitride thin films sputter-deposited on polished silicon ($R^2 = 0.984$); b) silicon carbon-nitride thin films sputter-deposited on polished silicon ($R^2 = 0.99$).

side of the silicon solar cell. For both applications, the uniformity of the thin film layer is crucial for the performance of the cell [10].

Thin films of silicon nitride ($\text{SiN}_x\text{:H}$) and silicon carbon-nitride ($\text{SiC}_x\text{N}_y\text{:H}$) were deposited by reactive sputtering process using a PlasmaQuest HiTUS deposition system [11]. The silicon nitride ($\text{SiN}_x\text{:H}$) and silicon carbon-nitride ($\text{SiC}_x\text{N}_y\text{:H}$) were deposited on polished silicon wafers. The deposition was carried out using metal targets (silicon and silicon/graphite 4:1 surface ratio respectively). The films were deposited in a mixed gas ambient of argon as a working gas and nitrogen and hydrogen as reactive gases forming hydrogenated nitrides at the surface of the substrates. Film properties were optimised for silicon solar cell applications and thickness was varied to investigate influence on thin film roughness and uniformity. The other deposition parameters were kept constant such as RF plasma launch power: 2.7 kW, target bias 0.9 kW, argon flow 50 sccm, nitrogen flow 5 sccm, hydrogen flow 5 sccm. The substrates were not heated for $\text{SiN}_x\text{:H}$ films. For $\text{SiC}_x\text{N}_y\text{:H}$ the other deposition parameters were kept constant at RF plasma launch power: 2.7 kW, target bias 0.9 kW, argon flow 50 sccm, nitrogen flow 5 sccm, hydrogen flow 5 sccm. The substrates were not heated during the deposition.

The transmission of silicon nitride and silicon carbon-nitride films deposited on glass was obtained using a spectrophotometer and these measurements are shown in Fig. 5. For these transmission measurements, the thickness of the silicon nitride thin film was ~ 210 nm and the thickness of the silicon carbon-nitride thin film was ~ 280 nm.

Both thin films show high optical transmission over the entire wavelength spectrum (200 nm–1400 nm). They absorb at ~ 350 nm and they show no interference fringes after 1250 nm.

The thickness measurements for both silicon nitride and silicon carbon-nitride thin films deposited on polished silicon again show good agreement between spectroscopic ellipsometry and the CCI techniques. The results show correlation with coefficient of determination R^2 of 0.984 for silicon nitride films and 0.99 for silicon carbon-nitride thin

films. The thickness range for the study is from ~ 65 nm to ~ 280 nm. The correlations are shown in Fig. 6.

The CCI technique was used to measure the roughness for all of the thin films of both $\text{SiN}_x\text{:H}$ and $\text{SiC}_x\text{N}_y\text{:H}$ (Fig. 7). The trend shows an increase of roughness with increased thickness, towards a plateau for a certain thickness (~ 150 nm for $\text{SiC}_x\text{N}_y\text{:H}$ and ~ 200 nm for $\text{SiN}_x\text{:H}$). The RMS roughness for both materials was < 2.5 nm for thin film thicknesses up to 150 nm. Thereafter, roughness increased with thickness with silicon nitride slightly rougher than the silicon carbon nitride. Even so, the RMS roughness of both materials did not exceed 5 nm.

8. Indium tin oxide

Indium tin oxide (ITO) is an important transparent conducting oxide widely used in applications such as touch screens, LCD and OLED displays, thin film photovoltaics ... [12]. It is usually composed of 90% indium oxide (In_2O_3) and 10% tin oxide (SnO_2). The films were deposited on soda lime glass using an AJA international Orion 8 sputtering tool. The ITO films were deposited using RF magnetron sputtering from an ITO target. A power of 150 W was applied to the target. The chamber was evacuated to a base pressure of $\sim 7.3 \cdot 10^{-5}$ Pa before the deposition. Argon was used as a working gas with the flow set to 7 sccm, the deposition pressure was kept constant during the deposition at 0.13 Pa. The glass substrate temperature during deposition was 400°C . The deposition time was varied to obtain increasing thin film thickness.

Optical transmission measurements were obtained from the ITO thin films and an example corresponding to a thin film thickness of 238 nm is shown in Fig. 8. The measurement shows high transmittance over the whole visible spectra with a steep decrease at 380 nm, due to the absorption of the photons with energy greater than the band gap. At higher wavelengths due to the high carrier concentration a decrease in transmittance is present around 1000 nm.

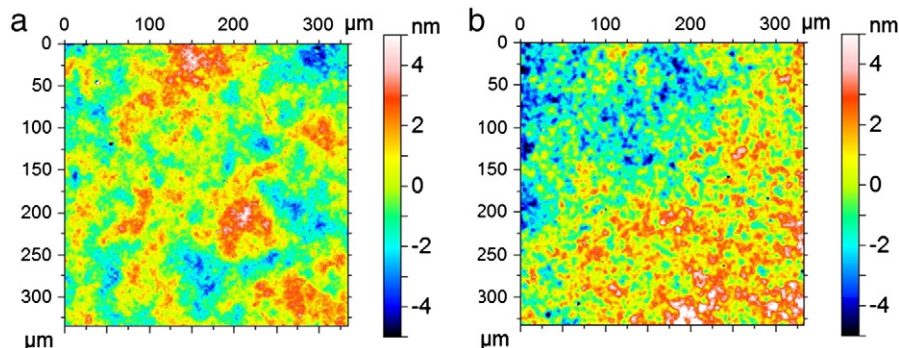


Fig. 7. A surface map – CCI image obtained from (a) 74.9 nm of SiN_x with RMS roughness of 1.51 nm; (b) 97.4 nm thin film of SiC_xN_y with RMS roughness of 1.78 nm.

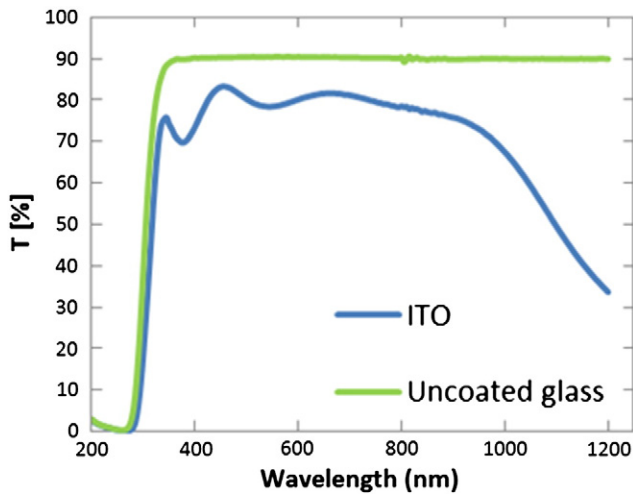


Fig. 8. The optical transmission spectra of a 238 nm thick indium tin oxide thin film deposited on glass.

Five ITO thin films of different thickness were sputter deposited on glass substrates. The thickness was measured using both CCI and spectroscopic ellipsometry. The correlation between the two methods is shown in Fig. 9.

The roughness of indium tin oxide films is important in many applications [13] such as displays and thin film photovoltaics since it is possible for this electrical conductor to make contact and short with layers above. Fig. 10 is a surface map of the 238 nm thick layer of ITO, sputter deposited on glass, with a sheet resistance of $6.2 \Omega/\square$. The ITO film is super-smooth and the RMS roughness is 0.92 nm.

The roughness of the ITO films increased with thin film thickness. The films thinner than 400 nm had a RMS roughness below 1 nm and even at 1 μm thickness the roughness was only ~ 1.5 nm. The deposited ITO films had sheet resistance in range between $13.7 \Omega/\square$ for 120 nm film and $1.4 \Omega/\square$ for 900 nm film.

9. Conclusions

Scanning White Light Interferometry is already an important technique used to provide three-dimensional surface metrology with a vertical resolution of 0.01 nm. It is a fast, non-contacting and hence

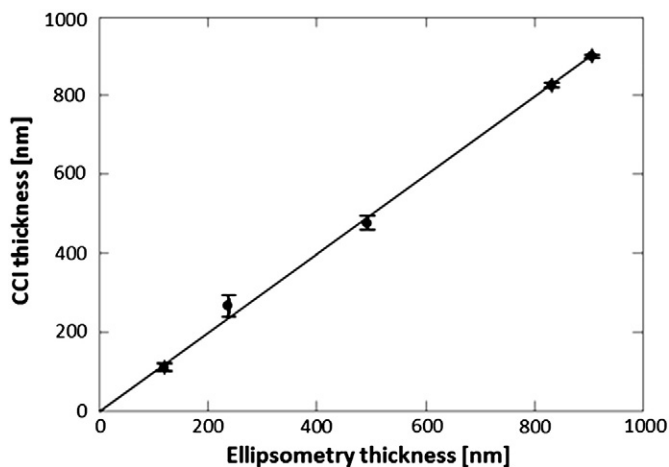


Fig. 9. Comparison between thin film thickness measurements obtained using ellipsometry and CCI techniques for indium tin oxide thin films sputter-deposited on glass ($R^2 = 0.997$).

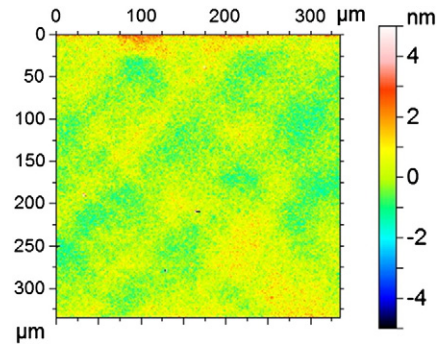


Fig. 10. A surface map – CCI image obtained from a 238 nm thin film of indium tin oxide. The RMS roughness parameter $S_q = 0.915$ nm.

non-destructive technique with widespread applications including the metrology of thin films. Previously the technique has been used to measure the thickness of transparent or semi-transparent coatings typically $> 1 \mu\text{m}$ thick. In this regime, two localized fringes appear each corresponding to the surface and the thin film-substrate interface. The thickness of the film is determined by locating the position of the two envelope maxima. However, for films of thickness $< 1 \mu\text{m}$ these fringes are overlapping.

The development of the helical complex field or HCF function now allows thin film thickness to be measured accurately provided the refractive index dispersion is known. In fact, the HCF function can also be used for thick films $> 1 \mu\text{m}$. In this study, we have tested the use of the HCF function on a range of important materials including metal oxides, nitrides, carbon-nitrides and transparent conducting oxides. In each case the measurements have also been carried out with conventional spectroscopic ellipsometry. We have shown that the correlation between the two thickness measurements for the two techniques is excellent.

Accurate measurement of the thickness of transparent and semi-transparent thin films is important in a number of applications including optical coatings, displays and transparent conducting oxides. The present authors have already applied the technique to thin film photovoltaics [14]. These measurements are currently made using spectroscopic ellipsometry or by a stylus profilometry that requires a step in the thin film for the measurement. In this paper we have shown that these measurements can now also be made using Coherence correlation interferometry (CCI) and the accuracy of the measurements is comparable with spectroscopic ellipsometry. Thickness measurements can be obtained automatically at various points on the sample surface using the 'pattern measurement' capability available for 'thin film' thickness measurements. This will be a useful tool for mapping thin film uniformity. Use of the HCF function provides a fast and straightforward method to determine thin film thickness, without the need for the presence of a step as is the case for profilometry or the use of complex models as used in ellipsometry.

Since the CCI is also capable of providing three-dimensional surface metrology, the thin film thickness capability made possible by the HCF function allows all these measurements to be made on the same sample area with sub-nanometre precision. This is a breakthrough in thin film measurement science and this combination of metrology capabilities will have important future use in a variety of applications.

Acknowledgements

The authors are grateful to EPSRC and TSB for funding. We are also grateful to Mr Daniel Mansfield and his colleagues at Taylor Hobson Ltd for the collaboration in this study and for funding a studentship for Biancamaria Maniscalco.

References

- [1] J. Biegen, Interferometric surface profiler, US Patent 4,869,593, vol. 2390676, 1989.
- [2] P.J. de Groot, X. Colonna de Lega, Proc. SPIE 7064 (Aug. 2008) 70640I.
- [3] D. Mansfield, Apparatus for and a method of determining surface characteristics, U.S. Patent WO/2007/0719442006.
- [4] D. Mansfield, Proc. SPIE 7101 (2008) 71010U.
- [5] D. Mansfield, Proc. SPIE 6186 (2006) 61860O.
- [6] Y. Yu, M. Conroy, R. Smith, Proc. SPIE 8417 (Oct. 2012) 84170H-1.
- [7] H.G. Tompkins, E.A. Irene, C. Hill, N. Carolina, Handbook of Ellipsometry, William Andrew Springer, 2005. 9–12.
- [8] A. Macleod, C. Clark, Optical Coating Design with the Essential Macleod, Thin Film Center Inc., Tucson, 2012.
- [9] D.R. Gibson, I. Brinkley, G.W. Hall, E.M. Waddell, J.M. Walls, Proc. SPIE 6286 (2006) 62860I.
- [10] M.A. Green, IEEE Trans. Electron Devices 420 (10) (1999) 3.
- [11] P. Kaminski, K. Bass, B. Maniscalco, J. Walls, G. Claudio, Proc. of 26th European PV Solar Energy Conference, 2011, p. 1766.
- [12] J.M. Nel, H.L. Gaigher, F.D. Auret, Thin Solid Films 436 (February) (2003) 186.
- [13] R.N. Joshi, V.P. Singh, J.C. McClure, Thin Solid Films 257 (1) (Feb. 1995) 32.
- [14] B. Maniscalco, P. Kaminski, J.M. Walls, Proc. of 38th Photovoltaic Specialists Conference, 2012, p. 417.